Grasping for the Seabed

Developing a New Underwater Robot Arm for Shallow-Water Intervention

By José Javier Fernández, Mario Prats, Pedro J. Sanz, Juan Carlos García, Raul Marín, Mike Robinson, David Ribas, and Pere Ridao

A new underwater robot arm was developed through intensive cooperation between different academic institutions and an industrial company. The manipulator, which was initially designed to be teleoperated, was adapted for our autonomy needs. Its dimensions and weight were reduced, and its kinematic model was developed so that autonomous control can be performed with it. We compare several commercially available underwater manipulators and describe the development of the new one, from its initial configuration to its mechanical adaptation, modeling, control, and final assembly on an autonomous underwater vehicle (AUV). The feasibility and reliability of this arm is demonstrated in water tank conditions, where various innovative autonomous object-recovery operations are successfully performed, both in stand-alone operation and integrated in an AUV prototype.

Underwater Manipulation

In the general context of robotics, grasping and manipulation remain open research problems. This situation becomes drastically worse in underwater scenarios, where new complexities arise and increase the difficulty of any physical interaction with the environment. The unmodeled underwater currents introduce continuous and unexpected motion disturbances that strongly affect any manipulation action. Under these very hostile conditions, only a few robot systems are endowed with semiautonomous manipulation capabilities, mainly focused in specialized operations requiring a reasonably structured environment, like those devoted to the offshore industries. In most cases, hydraulic-powered manipulators controlled remotely by expert pilots from a surface vessel are used. Most of these underwater arms have considerable dimensions and weight, and they require expert operators for their use.

The earlier achievements in the field of underwater intervention date back to the 1990s, when the UNION project [1] validated, in simulated conditions, coordinated control and sensing strategies to increase the autonomy of intervention remote-operated vehicles (ROVs). Simultaneously, the European project AMADEUS [2] demonstrated the coordinated control of two 7 degrees of freedom (DoF) arms submerged in a water tank. It was not until the turn of century that the first field interventions were demonstrated. SWIMMER [3] introduced a hybrid system in which an AUV was in charge of transferring a work ROV to a subsea site and connecting it to the site's communication tether, allowing the remote control of the vehicle. Later, the ALIVE project [4] demonstrated the capability of autonomously navigating, docking, and operating an underwater panel. From the control point of view, simulation experiments on redundant motion planning and tracking

Digital Object Identifier 10.1109/MRA.2013.2248307

Date of publication: 9 October 2013

1070-9932/13/$31.00©2013IEEE

Table 1. Commercial underwater lightweight arms.

Supplier	Model	Air Weight (kg)	Water Weight (kg)	Reach (mm)	Depth (m)	DoF	Power Technology
Hydro-lek	HLK-MB-4	–	16	806	2,000	4	Hydraulic
	HLK-EH5	10.5	8	795	–	5	Hydraulic
	HLK-HD5	21.5	16.5	819	–	5	Hydraulic
	HLK-RHD5W	30	20	943	–	5	Hydraulic
	HLK-HD6R	29	21	1,120	–	6	Hydraulic
	HLK-HD6 B	27	20	1,535	–	6	Hydraulic
	HLK-CRA6	28	14.5	1,500	–	6	Hydraulic
	HLK-40500	45	32	1500	–	7	Hydraulic
Int. Submarine Engineering	Magnum-5 Mini	13	–	711.2	–	5	Hydraulic
Kraft TeleRobotics	Grips	59	41	1,566	3,000	6	Hydraulic
CSIP	ARM 5E	27	18.5	1,044	3,000	5	Electric
Schilling Robotics	ORION 4R	30	21	682	6,500	4	Hydraulic
	ORION 7R	54	38	1,532	6,500	7	Hydraulic
	ORION 7P	54	38	1,532	6,500	7	Hydraulic
Western Space and Marine	MK37	43	16	940	6,000	7	Hydraulic
Ansaldo (SAUVIM Project)	MARIS 7080	55	–	1,400	6,000	7 + 1	Electric
Mitsubishi Heavy Industries (UNION Project)	PA10-7C	40	–	1,317	IP54	7	Electric
	PA10-6C	38	–	1,317	IP54	6	Electric
	PA10-300	35	–	1,345	IP54	7	Electric
	PA10-400	35	–	1,345	IP54	7	Electric

control under disturbances were performed [5]. In fact, few practical setups have been reported, and they are normally reproduced only on simplified environments. As described in [6], interesting results might be achieved through fully actuated AUVs carrying multi-DoF manipulators. Here, it is worth mentioning the SAUVIM project [7], which recently demonstrated the autonomous recovery of seafloor objects with a 7 DoF arm, and the CManipulator project [8], which has obtained interesting results on autonomous object grasping and connector plugging. In all of these, it is assumed that the object to grasp is known in advance in terms of a three-dimensional (3-D) model or special visual features.

This article presents a new lightweight underwater robot arm designed (although not limited) to be integrated in a new AUV, both constructed under partial support of the Spanish Coordinated Research Project RAUVI [9]. The objective of the RAUVI project (completed in December 2011) was the construction of a new lightweight AUV ready for autonomous intervention missions. The new AUV prototype, named GIRONA 500 [10], was conceived prior to designing the robot arm and, therefore, the physical constraints of this vehicle determined the guidelines to be followed in the arm mechatronics implementation. Because of the limited available time and financial resources, the best option was to look for an existing prototype in the market with an intention to adapt it in a suitable manner to the specific constraints imposed by the GIRONA 500 vehicle. This article describes the development process and the first experiments carried out with the new robot arm. More specifically, this article details how an electric manipulator initially designed for teleoperation with ROVs is adapted and enabled for autonomous intervention missions and how this step allows the execution of underwater tasks never done before.

Another contribution of this article is an updated comparison of different underwater manipulators commercially available on the market. To the best of authors' knowledge, the most recent comparison was by Yuh [11] in a survey on AUVs that included a section specifically devoted to mechanical manipulators. This article presents an update of the state of this technology (see Table 1).

The Arm Design Process

The Intervention-AUV Requirements

The characteristics of the AUV in which the manipulator is to be assembled (the GIRONA 500 AUV [10]) determined most of the requirements for the robot, which are the following:

- The robot arm should be able to reach the seafloor with the AUV hovering at a minimum altitude of about 50 cm.
- Each mobile part of the arm should be neutrally buoyant to reduce dynamic disturbances on the vehicle.

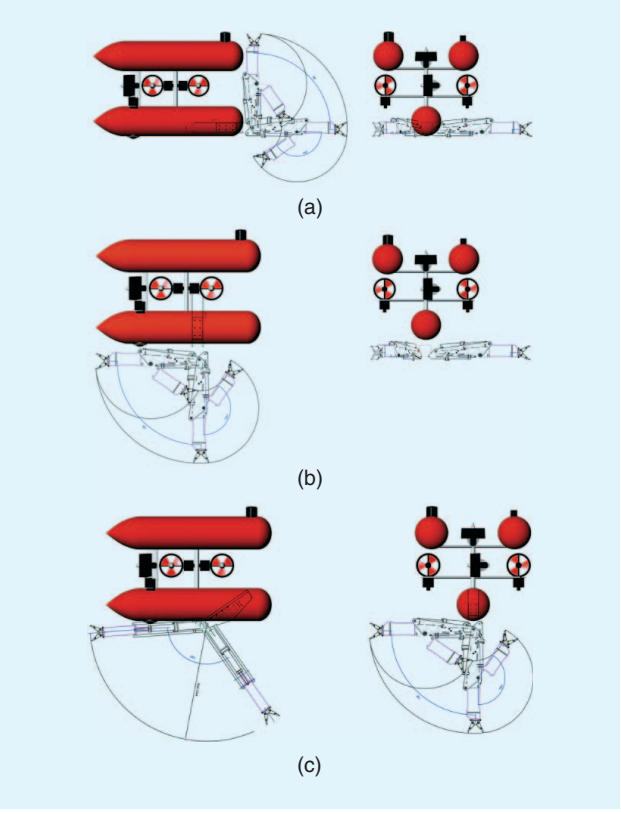

Figure 1. GIRONA 500–ARM 5 E assembly options. (a) Option 1, the arm is placed in the front of the vehicle. (b) Option 2, the arm is placed facing downward in the center of the vehicle. (c) Option 3, the arm is placed facing downward in the center of the vehicle but with the base in a slanted position.

- The arm should be as slender and lightweight as possible to be only a small part of the total intervention-AUV (I-AUV) weight and, therefore, reduce the dynamic coupling between both subsystems. If the mass of the vehicle is around 200 kg in air, the robot arm weight in air should not be >30 kg.
- The AUV elements should be out of the arm workspace to avoid damages on failure of its autonomous control. When not operative, the arm should adopt a position that minimizes the water resistance while the vehicle moves through the water.
- The arm should be attached to the payload area of the vehicle. To balance the vehicle, it is important to place the arm as close as possible to the center (this would vertically align the center of buoyancy and the center of gravity) and as low as possible (this would increase the distance between the buoyancy and gravity centers and improve the stability).
- Low power consumption is required, as the arm has to be connected to the vehicle batteries, and the time for autonomous operation has to be maximized.
- It is not required that the arm has a high payload. On the contrary, a small payload is preferred to reduce size and power consumption.

Table 2. Advantages and drawbacks of the GIRONA 500–ARM 5 E assembly options.

Option	Advantages	Drawbacks
Option 1: The arm is placed in the front of the vehicle	• Good for manipulating objects on the front of the vehicle • Free space for the control electronics cylinder	• The arm is placed very far from the center of the vehicle • Bad for manipulating objects below the vehicle (vehicle should be very close to the bottom)
Option 2: The arm is placed looking down in the center of the vehicle	• Good for manipulating objects on the bottom of the vehicle • Free space for the control electronics cylinder • The arm is placed almost at the center of the vehicle and as low as possible	• The base of the arm exceeds the limits of the hull
Option 3: The arm is placed looking down in the center of the vehicle but with the base in a slanted position	• Good for manipulating objects on the bottom of the vehicle • The base is placed inside the hull • The arm is placed almost at the center of the vehicle and as low as possible	• The assembly is more difficult • Little space for the control electronics cylinder

Underwater Robot Arms Technologically Available

In the search for an underwater arm with the above requirements, Table 1 was developed (November 2009). Only arms that were available at the time and that were close to the weight and reach requirements were included in the table. Although significant advances in hydraulic actuation technology were carried out during the last several years, electrical technology was ultimately chosen because of its higher accuracy and the possibility of directly connecting to the AUV power supply, reducing weight and volume. Among all the available options, the CSIP ARM 5 E manipulator was selected and later adapted to better suit our needs. This led to the new Light-Weight ARM 5 E presented in this article.

Possible Configurations of the GIRONA 500 and ARM 5 E

After selecting the CSIP ARM 5 E, the most suitable assembly configuration on the vehicle was analyzed to fulfill the GIRONA 500 and intervention requirements. Three options (illustrated in Figure 1) were analyzed. Their respective advantages and drawbacks are described in Table 2. The second option

was selected because of its clear advantages and relatively minor drawbacks.

Adaptation of the CSIP ARM 5 E

The weight of the original CSIP ARM 5 E was still too high, from a control point of view, to be directly attached to the vehicle. If the arm weight is a high percentage of the vehicle weight, considerable dynamic coupling between both subsystems would be introduced. To avoid such coupling, a light-weight version was developed in cooperation with the CSIP company, United Kingdom. This effort led to the new Light-Weight ARM 5 E. Oil compensation was removed, as it was not completely necessary for the maximum depth of 300 m considered in our projects. The link materials were also adapted and covered with foam to increase buoyancy. All these actions resulted in reduced arm weight. The final prototype and its main characteristics are described in the following section.

The CSIP Light-Weight ARM 5 E

The Light-Weight ARM 5 E is an underwater robotic manipulator powered by 24-V brushless geared dc motors. It is composed of four revolute joints and can reach distances up to 1 m. An actuated robot gripper allows small objects to be grasped, and its T-shaped grooves also permit the handling of special tools. The arm is made up of aluminum alloy partially covered with foam material to guarantee suitable buoyancy. The total weight in the air is ~29 kg (including the electronics cylinder), whereas in fresh water it decreases to ~12 kg. Table 3 shows the weights of each part of the arm without considering the electronics cylinder. The last row shows the total mobile mass. The fixed mass is within the vehicle payload and has little effect on vehicle stability. With a total weight in water of 8.95 kg, the original arm weight was reduced by around 50%.

The arm is capable of lifting 12 kg at a full reach (the original arm had a payload of 25 kg), and can descend up to 300 m in water. An underwater camera can be mounted either on the forearm or on the base link to provide a top view of the manipulation area. In our case, a Bowtech DIVECAM-550C-AL high-resolution color charge-coupled device camera, rated up to 100-m depth, is assembled. A complete datasheet of the new arm can be found on the CSIP Web site (www.csip.co.uk).

Figure 2 shows a computer-aided design (CAD) model of the Light-Weight ARM 5 E and its DoF. With the exception of the wrist rotation, the rest of joints are actuated by a prismatic mechanism, where the stroke of a cylinder generates a joint rotational motion. Table 4 shows some details of the motors and the actuation system, together with the range of each joint. The high reduction ratio of the joints makes the motor velocities significantly higher than the joints' velocities, thus decreasing the effect of coupled torques between joints. So we can consider the robot as *N* decoupled single-input, single-output subsystems and control each joint by conventional PID **<AU: Please spell out PID.>** design. Furthermore, the high reduction ratio also makes them keep

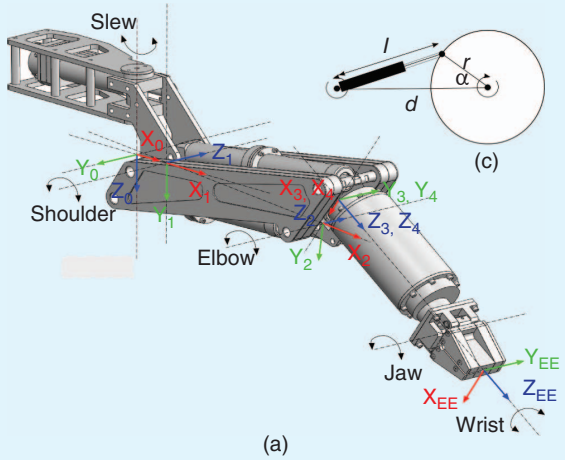

Link	θ (°)	d (mm)	a (mm)	α (°)
1	0	0	80.52	90
2	5	0	442.78	0
3	115	0	−83.00	90
4	0	0	0	0
EE	0	499.38	0	0

(b)

Figure 2. The CSIP Light-Weight ARM 5 E kinematic model. (a) Denavit–Hartenberg (D–H) reference frames. (b) D–H parameters. (c) Joint actuation model.

their position when the arm is not powered underwater. At normal operation (motor velocities of up to 2,000 r/min in the water and without load), the total current consumption is normally <25 W.

It is worth mentioning that all the housings are air filled at 1 atm with no oil present within the system. This has zero pollution risk, with no oil entering the environment in the event of accidental damage during the mission. With no hydraulics involved, this is a unique system.

The arm's low-level control and power electronics are placed in a housing cylinder that uses a PIC microcontroller to: 1) send/receive RS232 data packages to/from the control PC and 2) communicate with each motor microcontroller through a controller area network (CAN) bus. The RS232 communication protocol includes fixed-length motor command and sensor messages. Motor command messages are

Table 3. Main components' weights.

Components	Air Weight (kg)	Fresh Water Weight (kg)
Slew actuator and mounting assembly	7.8	5.15
Upper arm	9.8	2.0
Jaws and lower arm	7.4	1.8
Total mass	25	8.95
Total mobile mass	17.2	3.8

Table 4. Motors and drives.

Actuator	Range	Rated Speed (r/min)	Reduction Ratio	Ball Screw Lead (mm/rev)	Stroke (mm)
Slew	120°	4,000	56−1+ 27−33	8	100
Shoulder	85°	4,000	116−1	8	100
Elbow	130°	4,000	91−1	8	100
Wrist	Continuous	4,200	91−1+ 24−33	—	—
Jaw full open	150 mm between tips	4,200	24−1	2	19

sent from the PC to the arm and can be either a control demand in terms of position, speed or voltage, or a PID setting message. When the arm microcontroller receives a motor command message, it performs the corresponding control action and sends back to the PC a sensor message including the position, speed, current, and temperature of each motor as measured by the internal sensors. More details on the control architecture are given in the section "Control Software Architecture."

CSIP Light-Weight ARM 5 E Modeling

Figure 2 shows the geometric model of the Light-Weight ARM 5 E, together with the Denavit–Hartenberg (D–H) parameterization of the model. The arm is composed of a total of 5 DoF, and the first four are denoted as slew, shoulder, elbow and wrist, whereas the last one (jaw) is the gripper

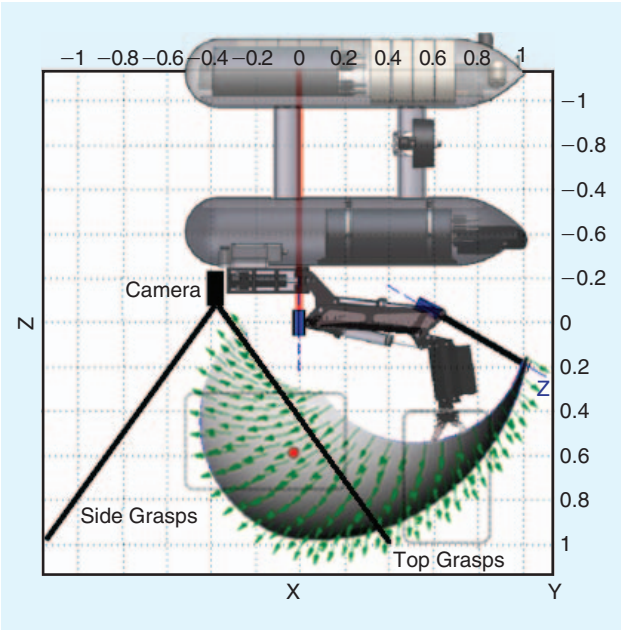

Figure 3. The arm workspace with the end-effector Z-axis over the workspace. Grayscale indicates the manipulability index.

actuation system that simply opens and closes the jaw without affecting to the end-effector pose. All the joints are rotational, although actuated with prismatic mechanisms. The only exception is the wrist rotation that is directly actuated through the gear train.

Workspace and Manipulability

A planar projection of the manipulator workspace when mounted in the vehicle is shown in Figure 3. It also shows the end-effector Z-axis at sampled points on the workspace. For the particular configuration of this arm, the end-effector Z-axis indicates the direction through which the target object would be reached if placed at that point in the workspace (due to the reduced number of DoF of the arm, the hand orientation can not be controlled at a given point in the workspace). It can be observed that the most suitable area for manipulation is around 60 cm below the arm base link (marked as a red circle in Figure 3). This area guarantees the highest distance to the workspace limits. The end-effector Z-axis in this area is almost horizontal, thus indicating that the most suitable approaching direction for grasping with this arm is from the side. Please note that top grasps are quite limited with this arm in the current configuration. Top grasps could only be performed on the rightmost area of the workspace, where the motion range is quite reduced. The workspace in Figure 3 also illustrates in grayscale intensity the volume $w_1 = \sqrt{\det(\mathbf{J}\mathbf{J}^T)}$ of the arm manipulability ellipsoid [12], $\mathbf{J}$ being the arm jacobian. Lighter gray indicates higher volume and, thus, higher manipulability. It is worth mentioning that the whole workspace of the arm is free of singularities.

As can be deduced from Figure 3, the most suitable position for placing an external camera is next to the arm base link and facing downward. This configuration guarantees that there is an intersection between the camera field of view and the arm workspace, allowing the arm to be controlled visually during execution of the task.

Arm Odometry

Hall-effect sensors are integrated into the arm motors, thus providing very basic position information. Each motor shaft revolution corresponds to eight position ticks that are measured with the hall-effect sensors and sent through the RS232 channel to the control PC. These position ticks are relative to the moment where the arm is powered; they do not provide absolute position feedback. It is therefore necessary to relate position ticks with respect to an absolute reference and convert position ticks to actual joint angles and vice versa.

If an absolute position measure with respect to the limits is available (because of an initialization procedure), this measure (hall-effect sensors position ticks) is transformed into actual joint angles (radians). This is done by first computing each actuator stroke (mm) according to the parameters of Table 4, and then computing the real angle through each joint actuation model. The general joint actuation model is

illustrated in Figure 2. There is a piston with a variable stroke of total length l, computed from the hall-effect sensors. The joint rotation origin is separated from the piston rotation axis a distance d, known from the CAD model. Finally, the end of the piston is attached to the joint at distance r, also known, from the joint rotation axis. Knowing these parameters, direct and inverse position and velocity models are derived.

Control Software Architecture

The low-level control architecture is implemented in C++, which makes use of the Robot Operating System (ROS) [13] for intermodule communications. At the lowest level, a communications module is in charge of receiving and sending RS232 data packages to the robot according to the communication protocol outlined in the section "The CSIP Light-Weight ARM 5 E." Other modules interact with this one to send control signals and process sensor data. More specifically, the following modules are involved (illustrated in Figure 4):

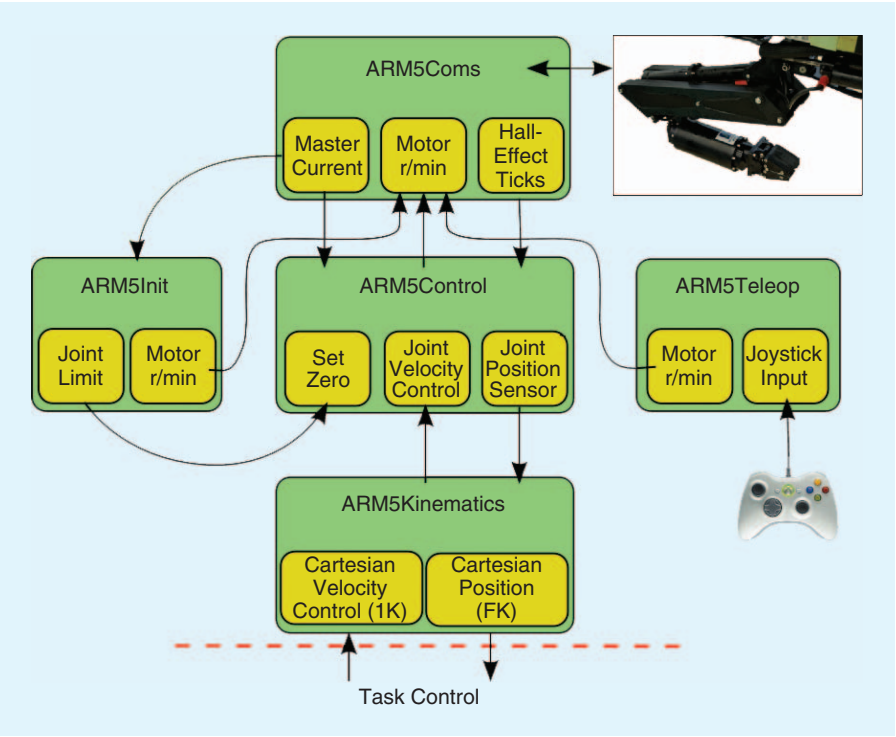

Figure 4. The different modules that compose the low-level control architecture.

- *ARM5Coms*: This module constantly sends a motor velocity control signal (in revolutions per minute) to each joint of the robot via a RS232 package. It waits until the manipulator controller sends back another data package with sensor information. The sensor data include master current, each joint current, and the ticks sensed by the hall-effect sensors of each motor. These data are suitably processed and made available to the rest of modules via ROS topics. Similarly, other modules can indicate the velocity reference that will be sent to the joints. The RS232 communication channel runs at 80 Hz.
- *ARM5Init*: This package performs the automatic initialization of the arm. It sequentially moves each joint toward the limit by sending a constant motor velocity to the ARM-5Coms module. Simultaneously, the ARM5Init module is constantly monitoring the master current sensor. When the master current is higher than a given threshold, the motor is stopped, and the *Set Zero* service of the ARM-5Control module is called, which is in charge of setting an absolute zero for each joint.
- *ARM5Teleop*: This module is used for arm teleoperation. It receives input from a joystick device and maps each joystick axis to one of the arm joints. Motor velocity is directly sent to the ARM5Coms module.
- *ARM5Control*: This module is in charge of providing a comprehensive view of the arm state to the rest of the architecture. First, it implements a virtual joint position sensor that transforms hall-effect sensors ticks into absolute joint angles, given with respect to the D–H model. In addition, it receives joint velocity references and transforms them into motor revolutions per minute that are sent to the communications module.
- *ARM5Kinematics*: Finally, the kinematics module computes forward and inverse differential kinematics of the arm from the D–H model. ARM5Kinematics is the interface with the high-level task control architecture, i.e., at a higher level, the arm is controlled in the Cartesian space, as will be shown in the experimental results.

First Experiments with the Light-Weight ARM 5 E

Different experiments are performed to test and validate the new arm in realistic conditions. First, it is installed in a water tank, attached to a fixed platform. With this setup, the initialization process and Cartesian control are tested. The manipulator is mechanically and electronically attached to an AUV, and the autonomous control and stability of the complete system are validated through an experimental benchmark: recovering a flight data recorder (FDR), commonly called a black box, from the bottom of a water tank.

Grasping with the Stand-Alone Arm Fixed in a Water Tank

Figure 5 shows the arm performing an autonomous grasping action in a water tank. The camera (situated next to the base link and facing downward) was capturing images and computing the pose of the box placed on the floor using

efficient second-order minimization (ESM) template tracking [14] and the Dementhon pose estimation algorithm [15]. The computed 3-D pose of the target is used to control the robot in Cartesian coordinates to reach and grasp the object. For that, a Cartesian velocity proportional to the error between the current end-effector pose and the desired grasp position is sent to the manipulator end-effector. The grasping action is performed when the end-effector is close to the reference position. It is noticeable that a 3-D representation of the task is needed for relating the visual template to the parts to be manipulated. Please refer to [16] for details on how to automatically generate such representation with a user interface.

These experiments with the fixed arm allowed the validation of the arm kinematic model and its autonomous control in the Cartesian space. It is difficult to assess the accuracy of the arm as there is no ground truth easily available. In addition, eye-hand calibration and visual pose estimation naturally introduce small errors. Therefore, it was decided to validate the arm and its controllers with an experimental benchmark never achieved before in an underwater scenario: introducing a hook in a handle in a complete autonomous way, with the manipulator attached to a floating vehicle.

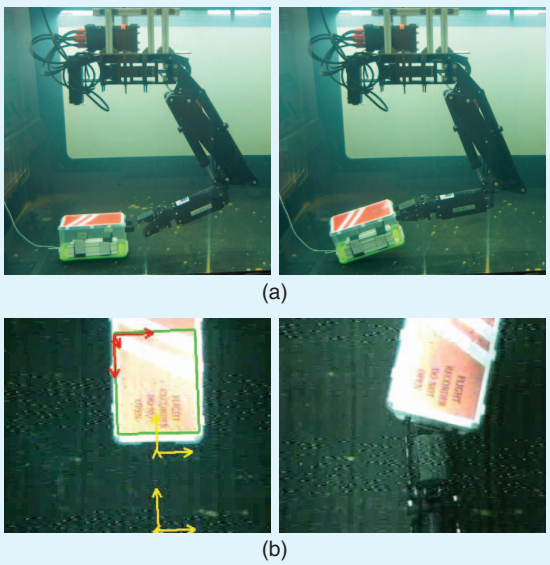

Figure 5. The grasping capabilities of the arm in autonomous mode on a fixed platform. (a) The underwater arm autonomously grasping a black box mockup. (b) Object tracking and grasping as seen through the top-mounted camera.

Integration with the GIRONA 500 AUV

Integration with the GIRONA 500 AUV [10] was carried out at the Centre d'Investigació en Robòtica Submarina (CIRS) water tank (University of Girona). In a first integration effort, the arm is mechanically attached to the GIRONA 500 AUV, the buoyancy of both subsystems is suitably adapted, and the first teleoperation results are obtained in the task of recovering an amphora. This experiment demonstrated the feasibility of the mechatronic integration and the possibility to teleoperate the arm for its use in ROVs.

In a second integration effort, the autonomous capabilities of the system are demonstrated in the task of searching and recovering an FDR from the bottom of a water tank (see Figure 6). The goal is to attach a hook to the handle of a mockup of the black box. It is worth noting the suitability of this benchmark for measuring the accuracy of the vehicle-arm control as the space of the handle for hooking is <3 cm [see Figure 6(a)]. The intervention is carried out as follows: first, the vehicle is placed on top of the FDR. Then, the task of the AUV is to keep its position and attitude with respect to the target object, guided by vision (visual station keeping). This is done by controlling the visual error (between current and desired object position in the image) to zero by using the vehicle thrusters. While station keeping, the arm end-effector is controlled toward the handle with visual feedback. It is able to autonomously hook the object in different trials. Several video sequences of these tasks can be found on the IRSLab YouTube channel [17].

Detailed results of these experiments are provided in [18]. Concerning arm control, successfully attaching a hook in different attempts demonstrates the accuracy of the arm and its autonomous control, especially accounting for the fact that the vehicle is floating during the task and, thus, under some motion. In addition, a vision error due to

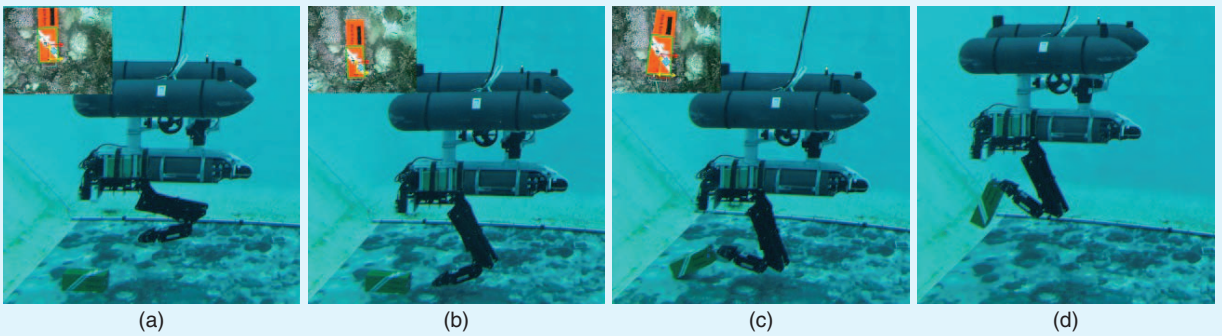

Figure 6. The grasping capabilities of the arm in autonomous mode mounted on an I-AUV. (a)–(d) From left, the arm is approaching the target while the vehicle performs station keeping. After retrieval of the target, the I-AUV returns to the surface.

tracking and pose estimation is also introduced in the loop. Even under these uncertainties, the hook is successfully attached in a space of <3 cm.

Figure 7 shows the Cartesian trajectory followed by the arm end-effector in one of the experiments, together with the initial configuration of the arm, plotted with the MATLAB Robotics Toolbox. The trajectory was divided in three parts by setting intermediate goal frames relative to the handle (denoted as *prehook* and *hook* frames). After estimating the pose of the object by vision, the intermediate frames relative to it are also instantiated with respect to the arm base, and, therefore, a Cartesian control of the end-effector can be performed proportional to the Cartesian error between the end-effector pose and the different set points. The motion disturbances detected on the vehicle are

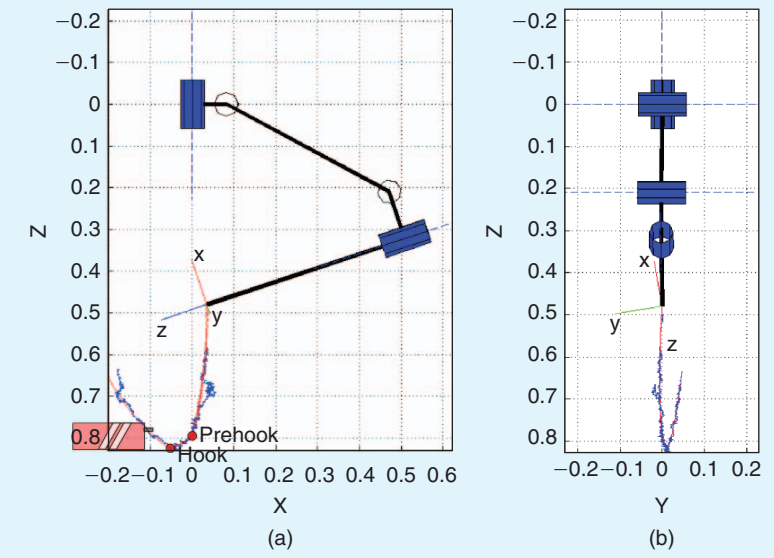

Figure 7. The trajectory of the ARM 5 E end-effector during the hooking action with respect to the arm base frame (red) and superposed with the motion disturbances of the vehicle under visual station keeping (blue). (a) Lateral view. (b) Front view.

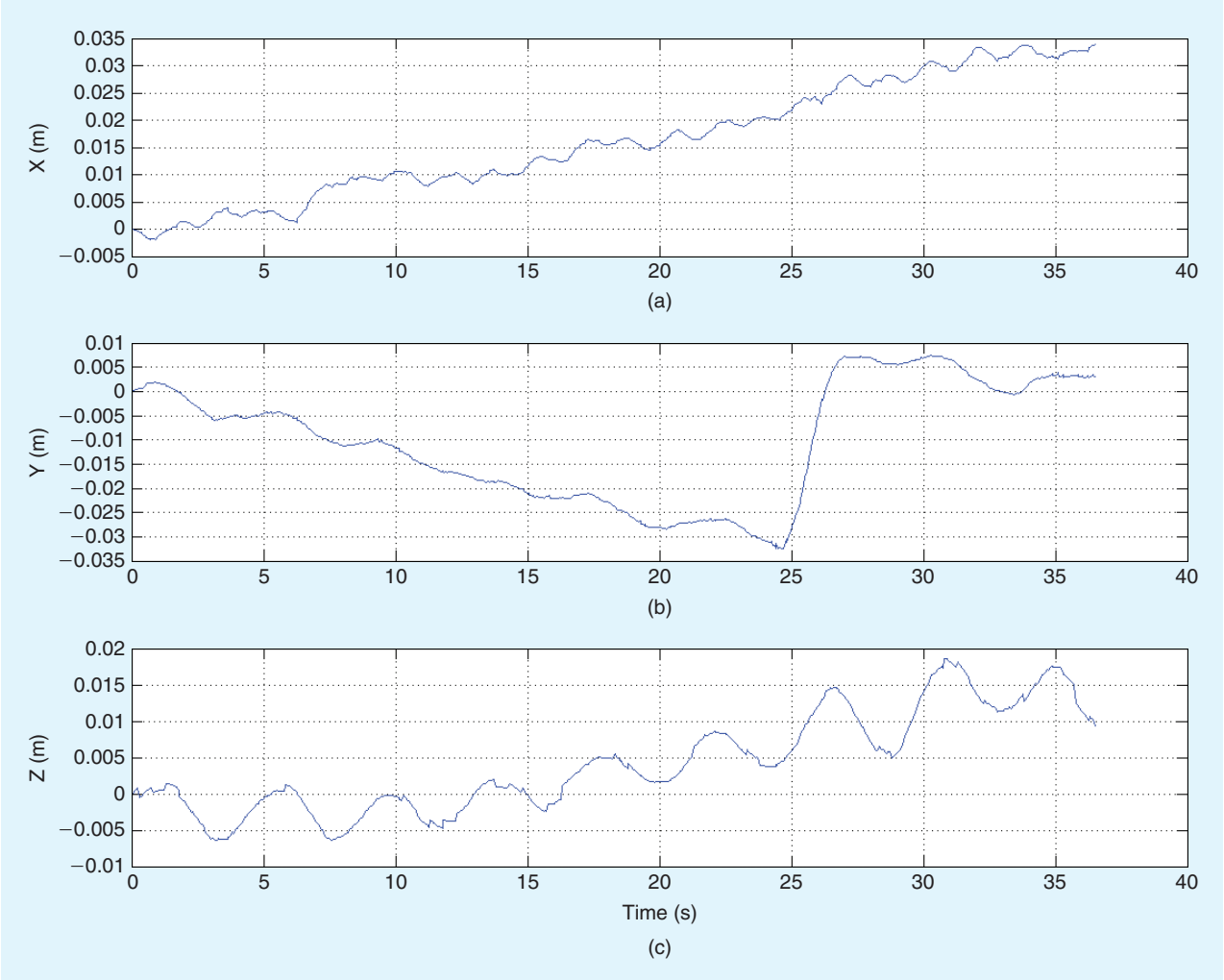

Figure 8. (a)–(c) Position disturbances measured at the base of the arm.

plotted in Figure 8. These correspond to the period when the vehicle was doing visual station keeping, and after the target object is centered on its desired position in the image.

Figure 9 shows the trajectory of the tracked object in camera coordinates, from its initial position to the final position where it is hooked. The initial position is far from the desired configuration, and, therefore, the vehicle moved to bring the black box handle toward a more appropriate pose. The small disturbances around the final configuration show the visual displacements that were detected (equivalent to those detected by the vehicle sensors and plotted in Figure 8) and used to: 1) keep the vehicle pose as much stable as possible on top of the target and 2) update the end-effector trajectory accordingly.

Discussion

This article describes an innovative implementation of an electric underwater manipulator mounted on an AUV. Autonomous control and manipulation capabilities are demonstrated through a practical scenario.

The autonomy levels accomplished in this research with the Light-Weight ARM 5 E manipulator, applied here to an AUV, could be also applied to ROVs. Certain tasks (or part of them) could be automated, thus simplifying the pilot task and requiring less expertise. In fact, the black box recovery task took around 4 min to perform in teleoperation (with a nonexpert pilot). The main problem is the difficulty of estimating the distance to the object from the camera perspective. The autonomous execution took only around 40 s.

The manipulation system is independent of a specific vehicle. Its basic version includes the arm and a container holding the power electronics. The external interface is a 12-pin standard connector that carries power, RS232 signals, and analog video of the onboard camera. For a complete autonomous use, another container with a control PC is required. The external interface includes a power connector (9–36 V) and an Ethernet connection that can be used for configuration or monitoring if needed. Therefore, the integration in different vehicles is straightforward, assuming that size and weight constraints are met.

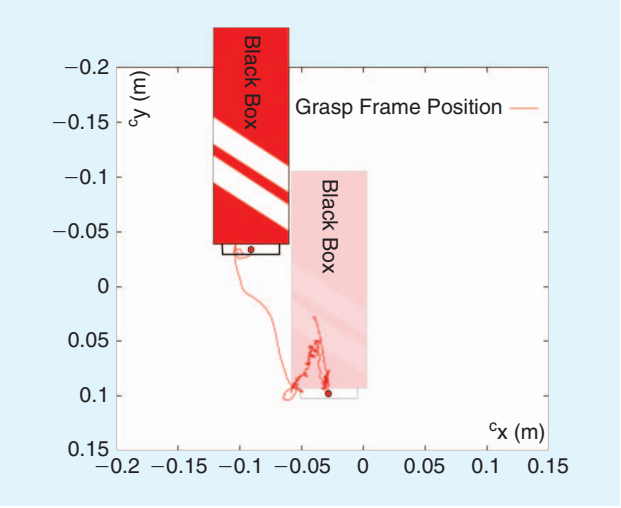

Figure 9. The visual evolution of the black box position during the intervention.

It is worth mentioning the kind of tasks that can be automated by the system herein described. In general, any task that requires a specific trajectory to be performed with the end-effector could be easily performed with the proposed system. If visual feedback is required (e.g., grasping, plugging a connector, etc.) the current vision system is limited to quasi-planar objects for which an appearance image is previously available or can be obtained before the intervention. This allows the specification in advance of the task. In the context of our projects, there is an intermediate step (between inspection and intervention) where real images of the site to manipulate are available and used for acquiring the target object appearance.

The decision concerning the arm and camera placement was a good solution. The I-AUV was very stable, with just a few centimeters of motion disturbances when the arm was moving (see Figure 8). However, high arm velocities were not considered in these experiments to minimize the dynamic coupling between the manipulator and the vehicle.

Finally, vehicle-arm coordinated motion is not addressed in this article, although it is one of the goals in our project [19] and will be considered in future work. As an intermediate solution, a station-keeping vehicle in a closed loop with visual feedback is considered.

Conclusions and Future Work

A new underwater robot arm was presented in this article. A continuous effort over a period of more than two years was necessary to achieve its complete functionality and its successful integration with a new AUV prototype developed under a Spanish coordinated project named RAUVI. We described the steps that were necessary to adapt the robot arm according to the initial requirements, and we also introduced its kinematic model that allowed autonomous control to take place. Different experiments carried out in a water tank object-recovery context demonstrated its feasibility and reliability. At this moment, autonomous control was performed using visual tracking and servoing techniques. Current research is focused on the integration of new contact-based sensors: a force/torque sensor and tactile pads would be a convenient combination to perform more robust autonomous underwater grasping and manipulation. Moreover, new grippers and robot hands (with more than two fingers) are now under exploration to provide improved dexterity and to progress toward multipurpose manipulation in underwater domains.

Since March 2010, the three-year project RAUVI, partially described in this article, became the core of a more challenging European project, named FP7-TRIDENT, which focuses on cognitive marine robotics for multipurpose intervention missions [20]. In addition, another Spanish coordinated and funded project, TRITON, was started in January 2012 with

the main purpose of applying the results of RAUVI to real autonomous intervention tasks at sea and eventually generating technological transfer.

Acknowledgments

This research was partly supported by Spanish Ministry of Research and Innovation DPI2011-27977-C03 (TRITON Project) and DPI2008-06548-C03 (RAUVI Project), by the European Commission's Seventh Framework Programme FP7/2007-2013 under grant agreement 248497 (TRIDENT Project), by Foundation Caixa Castelló-Bancaixa PI.1B2011-17, and by Generalitat Valenciana ACOMP/2012/252.

References

[1] V. Rigaud, E. Coste-Maniere, M. Aldon, P. Probert, M. Perrier, P. Rives, D. Simon, D. Lang, J. Kiener, A. Casal, J. Amar, P. Dauchez, and M. Chantler, "Union: Underwater intelligent operation and navigation," *IEEE Robot. Automat. Mag.*, vol. 5, no. 1, pp. 25–35, 1998.

[2] D. Angeletti, G. Bruzzone, M. Caccia, G. Cannata, G. Casalino, S. Reto, and G. Veruggio, "AMADEUS: Dual-arm workcell for co-ordinated and dexterous manipulation," in *Proc. OCEANS Conf.*, 28 Sept.–1 Oct. 1998, vol. 2, pp. 947–952.

[3] J. Evans, K. Keller, J. Smith, P. Marty, and O. Rigaud, "Docking techniques and evaluation trials of the swimmer AUV: An autonomous deployment," in *Proc. OCEANS*, 2001, pp. 520–528.

[4] J. Evans, P. Redmond, C. Plakas, K. Hamilton, and D. Lane, "Autonomous docking for Intervention-AUVs using sonar and video-based real-time 3D pose estimation," in *Proc. OCEANS*, Sept. 2003, vol. 4, pp. 2201–2210.

[5] J. Han and W. K. Chung, "Coordinated motion control of underwater vehicle-manipulator system with minimizing restoring moments," in *Proc. Intelligent Robots and Systems, IROS IEEE/RSJ Int. Conf.*, Sept. 2008, pp. 3158–3163.

[6] G. Antonelli, *Underwater Robots Motion and Force Control of Vehicle-Manipulator Systems* (Springer Tracts in Advanced Robotics), 2nd ed. New York: Springer-Verlag, 2006.

[7] G. Marani, S. K. Choi, and J. Yuh, "Underwater autonomous manipulation for intervention missions AUVs," *Ocean Eng.*, vol. 36, no. 1, pp. 15–23, 2009.

[8] D. Spenneberg, J. Albiez, F. Kirchner, J. Kerdels, and S. Fechner, "C-manipulator: An autonomous dual manipulator project for underwater inspection and maintenance," in *Proc. ASME Conf.*, vol. 2007, no. 42703, pp. 437–443.

[9] P. J. Sanz, M. Prats, P. Ridao, D. Ribas, G. Oliver, and A. Orti, "Recent progress in the RAUVI project: A reconfigurable autonomous underwater vehicle for intervention," in *Proc. 52nd Int. Symp. ELMAR-2010*, Zadar, Croatia, Sept., pp. 471–474.

[10] D. Ribas, N. Palomeras, P. Ridao, and M. Carreras, "Girona 500 AUV, from survey to intervention," *IEEE/ASME Trans. Mechatron.*, vol. 17, no. 1, pp. 46–53, 2012.

[11] J. Yuh, "Design and control of autonomous underwater robots: A survey," *Auton. Robot.*, vol. 8, no. 1, pp. 7–24, 2000.

[12] T. Yoshikawa, "Manipulability of robotic mechanisms," *Int. J. Robot. Res.*, vol. 4, no. 2, pp. 3–9, 1985.

[13] M. Quigley, B. Gerkey, K. Conley, J. Faust, T. Foote, J. Leibs, E. Berger, R. Wheeler, and A. Ng, "ROS: An open-source robot operating system," in *Proc. ICRA Workshop Open Source Software*, 2009.

[14] S. Benhimane and E. Malis, "Real-time image-based tracking of planes using efficient second-order minimization," in *Proc. IEEE/RSJ Int. Conf. Intelligent Robots Systems*, 2004, pp. 943–948.

[15] D. Dementhon and L. Davis, "Model-based object pose in 25 lines of code," *Int. J. Comput. Vis.*, vol. 15, no. 1/2, pp. 123–141, June 1995.

[16] M. Prats, J. C. García, J. J. Fernández, R. Marín, and P. J. Sanz, "Towards specification, planning and sensor-based control of autonomous underwater intervention," in *Proc. 18th IFAC World Congr.*, Milano, Italy, Aug. 2011, pp. 10361–10366.

[17] IRSLab. IRSLab YouTube Channel. [Online]. Available: http://www.youtube.com/IRSLab

[18] M. Prats, D. Ribas, N. Palomeras, J. García, V. Nannen, S. Wirth, J. Fernández, J. Beltrán, R. Campos, P. Ridao, P. J. Sanz, G. Oliver, M. Carreras, N. Gracias, R. Marín, and A. Ortiz, "Reconfigurable AUV for intervention missions: A case study on underwater object recovery," *Intell. Service Robot.*, vol. 5, no. 1, pp. 19–31, 2012.

[19] G. Casalino, E. Simetti, A. Turetta, and E. Zereik, "Distributed self-organizing control and coordination of cooperative mobile manipulator systems," in *Control Themes in Hyperflexible Robotic Workcells*, F. Basile and P. Chiacchio, Eds. Orlando, FL: CUES, July 2010, pp. 87–100.

[20] P. J. Sanz, P. Ridao, G. Oliver, G. Casalino, C. Insaurralde, C. Silvestre, C. Melchiorri, and A. Turetta, "TRIDENT: Recent improvements about autonomous underwater intervention missions," in *Int. Federation Automatic Control Workshop Navigation, Guidance Control Underwater Vehicles, IFAC,* Apr. 2012, pp. 355–360.

José Javier Fernández, Computer Science and Engineering Department, University of Jaume-I, Spain. E-mail: fernandj@uji.es.

Mario Prats, Computer Science and Engineering Department, University of Jaume-I, Spain. E-mail: mprats@uji.es.

Pedro J. Sanz, Computer Science and Engineering Department, University of Jaume-I, Spain. E-mail: sanzp@uji.es.

Juan Carlos García, Computer Science and Engineering Department, University of Jaume-I, Spain. E-mail: garciaju@uji.es.

Raul Marín, Computer Science and Engineering Department, University of Jaume-I, Spain. E-mail: rmarin@uji.es.

Mike Robinson, CSIP Ltd. United Kingdom. E-mail: mr@csip.co.uk.

David Ribas, Center for Underwater Robotics Research, University of Girona, Girona, Spain. E-mail: dribas@eia.udg.edu.

Pere Ridao, Center for Underwater Robotics Research, University of Girona, Girona, Spain. E-mail: pere@eia.udg.edu.